

Mechanical behavior of self-healed Ultra High Performance Concrete: from experimental evidence to modeling

S.Granger, G.Pijaudier-Cabot & A.Loukili
ERT R&DO, GeM, Ecole Centrale de Nantes, France

ABSTRACT: Self healing of cracks, in an ultra high performance concrete, is investigated in this paper, and especially the role of the phenomenon on mechanical properties. An experimental program is thus developed in order to characterize the mechanical behavior of prismatic specimens, initially cracked and then submitted to self healing, by total immersion in water. The most significant results are a fast recovery of global stiffness and a slight improvement of flexural structural resistance. Microscopic investigations are also proposed to qualify the nature of newly-formed crystals that precipitate in the crack. Then, a first approach of modeling of the mechanical behavior of concrete specimens, including the self healing process, is proposed. A coupling between hydration and elastic-damage models is thus developed and permits to get first qualitative results showing the experimental tendencies.

1 INTRODUCTION

Under special conditions and without any external intervention of repair, the phenomenon of self healing of cracks can appear and act positively on the durability and serviceability problems of concrete structures. The phenomenon is only possible in presence of water (dissolved CO_2 is not always needed) and consists of chemical reactions of compounds present on the crack surfaces. There are two major hypotheses regarding the chemical reactions (Neville, 2002): the hydration of anhydrous cement available in the microstructure of hardened concrete (especially for concrete with low Water to Cement (W/C) ratio), and the precipitation of calcium carbonate CaCO_3 (also called calcite) after the dissolution of portlandite (especially for concrete with high W/C ratio).

The majority of research works carried out on this topic highlights the phenomenon by means of water permeability tests. A decrease of flow rate through cracked specimens is the main method to show the self healing of cracks. Such tests have been carried out on concretes with high W/C ratio by Edvardsen (1999) or Hearn & Morley (1997), who show the precipitation of new calcite crystals. The influences of temperature and crack width have also been investigated (Reinhardt & Joos, 2003). The role of the phenomenon on transfer properties (see also, Jacobsen et al., 1996a, for chloride migration) has thus been fully characterized.

Concerning the mechanical impact, a few studies have been conducted. Jacobsen et al. (1996b) have shown a substantial recovery of frequency resonance on concrete cubes damaged by freeze/thaw cycles and then stored in water, but only a small recovery of compressive strength. SEM investigations have shown the precipitation of new C-S-H crystals (Jacobsen et al., 1995). Pimienta & Chanvillard (2004) also provide some insights about the mechanical properties of healed specimens. The authors reported that the frequency resonance of specimens damaged and then aged in water, tends to recover its initial value. Nevertheless, knowledge about the mechanical properties is scarce, and this contribution aims at providing some new insights about the mechanical behavior of healed concrete specimens.

An experimental program is developed on an ultra high performance concrete. Prismatic notched specimens are cracked under three-point bending (different types of residual crack width) and then totally immersed in water for different ageing times. After this ageing phase, the mechanical behavior of the healed specimens is characterized by means of three-point bending tests, and compared with the mechanical behavior of non healed cracked specimens. This characterization is completed by microscopic investigations in the zone of the pre-existing crack. All these results enable to provide a first approach of modeling of the mechanical behavior of the healed specimens, by coupling hydration and elastic-damage models. Simulations of the three-point bending tests are thus proposed.

2 THE MECHANICAL CHARACTERIZATION

2.1 Concrete specimens

The experimental program is carried out on an ultra high performance concrete (UHPC). This concrete is characterized by a low W/C ratio, close to 0.2. This implies that the amount of anhydrous clinker in the microstructure is very high, in the order of 50% (Loukili et al., 1998). The composition of this concrete is composed of sand, water, cement, silica fume and a superplasticizer, but no coarse gravels. This UHPC has a quite homogenous microstructure with a high amount of anhydrous clinker, and thus a high potential for self healing by hydration of this cement.

In order to have a localized crack during the mechanical tests, a notch of depth 20 mm and thickness 1.5 mm is performed in each specimen (dimensions 50x100x500 mm). After casting, the concrete specimens are cured for 2 days at 20°C and 100% relative humidity. A thermal treatment is then applied, so as to accelerate hydration, to activate the pozzolanic reaction, and to get chemically stable concrete. The specimens are placed in a climate chamber with a controlled environment of 90°C and 100% relative humidity during 48 hours.

2.2 Mechanical tests

During the first phase of the mechanical program, specimens are loaded under three-point bending in order to be cracked (Figure 1). The tests are crack opening controlled with a constant rate of 0.05 $\mu\text{m/s}$. The aim of this first step is to get a controlled cracking of the specimens. Pre-cracking is performed in the post peak regime: after having reached the peak load, specimens are unloaded at different stages in order to get residual crack widths of respectively 10, 20 and 30 μm . This unloading is also crack opening controlled with the same rate as loading.

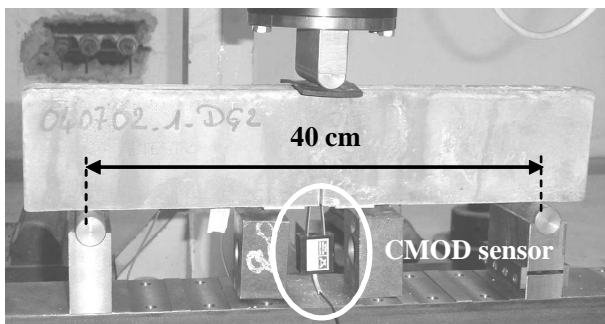


Figure 1. Mechanical test configuration

After this first step, the specimens are stored in specific conditions for ageing. There are two kinds of ageing: in air at 20°C and 50% relative humidity, and in total immersion in tap water, without movement neither renewal. For specimens cracked with

residual crack widths of 10 μm , the different periods of ageing are 1, 3, 10, 20 and 40 weeks, in order to analyze the influence of ageing time. The influence of cracked width is studied with the complementary results of specimens cracked at 20 and 30 μm , and aged for 10 and 20 weeks.

After this ageing phase, the last step of the experimental program consists in reloading the specimens under three-point bending, so as to characterize their residual mechanical behavior. Tests are also crack opening controlled and conducted until total failure.

2.3 Mechanical behavior of aged specimens

Figure 2 presents the mechanical behavior of specimens that have been aged in water for 1, 3, 10 and 20 weeks, after having been pre-cracked with a residual crack width of 10 μm . These are average curves (three tests for each kind of ageing). The initial value of the crack opening has been shifted to zero, in order to have the same initial state, but in reality there is still the value of the residual crack opening. These results are compared to the average mechanical behavior of specimens stored in air, which is the same as those of non aged cracked specimens (Granger et al., 2006). The curves display the crack opening versus the ratio between load applied and load while unloading in the pre-cracking phase.

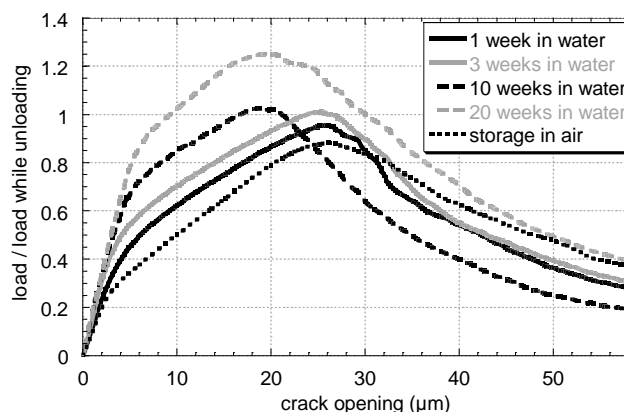


Figure 2: Mechanical behavior of aged cracked specimens

These results show the evolution of the mechanical behavior with the time of storage in water. The initial reloading stiffness is not the same as for non aged specimens, and it increases with the ageing time. There is also a slight improvement of flexural strength and a change in stiffness (limit of the elastic phase) in the pre peak regime, which evolves with time, and should be associated with an evolution of the mechanical characteristics of the healed zone of the specimen.

Figure 3 represents the evolution of the ratio between the reloading stiffness with healing, and the reloading stiffness without healing, as a function of the ageing time.

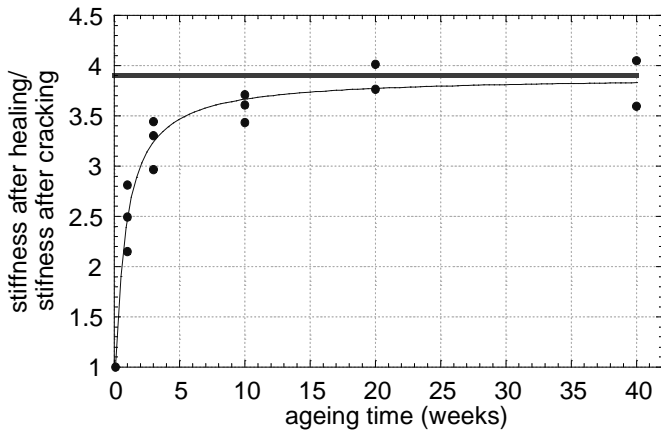


Figure 3: Evolution of the ratio between the stiffness with healing and the stiffness without healing – Comparison with the average ratio of healthy specimens

It is noticeable that there is a fast recovery of the structural stiffness by self healing, and this stiffness tends to the one of healthy specimens, which is represented by the straight line on the graph. Figure 4 now shows the evolution of the ratio between peak load after ageing and load measured upon unloading prior to ageing. We can thus notice that there is a slight improvement of the flexural resistance in comparison with the healthy specimens, and that the resistance of initial undamaged specimens can not be achieved after self healing.

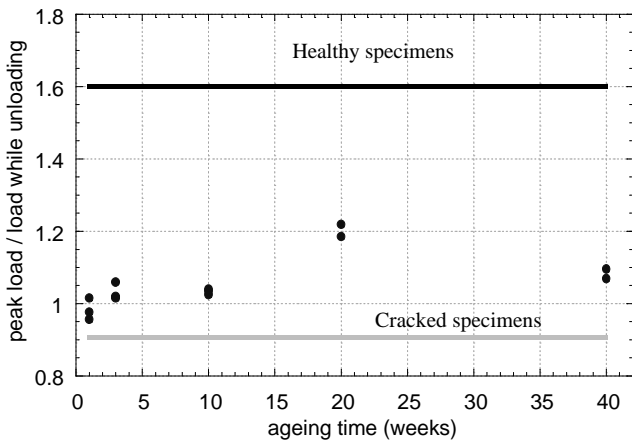


Figure 4: Evolution of the ratio between peak load and load while unloading prior to ageing, for healed specimens, in comparison with cracked and healthy ones

The influence of the crack opening has also been investigated. Figure 5 shows the global stiffness during the reloading phase as a function of the residual crack opening got at the end of the pre-cracking phase. The results for 10 and 20 weeks of ageing are presented.

So, there is a clear influence of the residual crack opening on the stiffness while reloading. We can thus notice, like on figure 3, that, for specimens cracked at 10 μm , the recovery of stiffness is complete. In comparison, this is not the case for speci-

mens cracked at 30 μm , even for 20 weeks ageing which is quite a long period for the concrete studied.

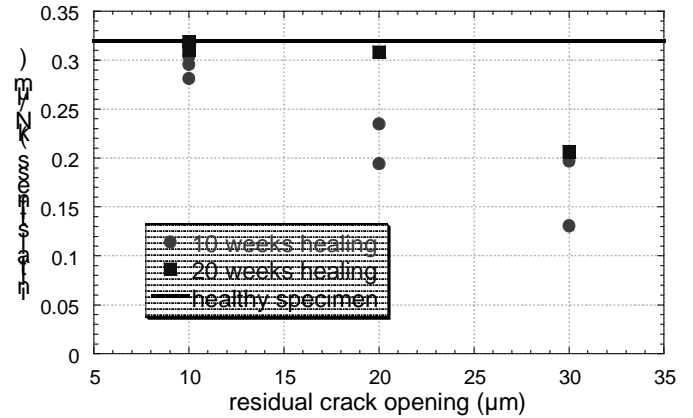


Figure 5: Evolution of the global stiffness for different residual crack openings, compared with the average stiffness of healthy specimens

2.4 The precipitation of crystals

The two most important mechanical results presented in the previous section, are attributed to the phenomenon of self healing, by precipitation of new crystals in the crack. An acoustic emission analysis of the cracking processes of the specimens, during the reloading phase after ageing, has been conducted (Granger et al., 2006). It shows that the damage of specimens stored in water begins sooner than those of non healed beams, and that the micro-cracks detected are located in the zone of the pre-existing crack. The analysis of the dissipated acoustic energies also shows that the newly formed crystals seems to be less resistant than C-S-H from the first hydration. In order to get more information about their nature, and to make a link with the mechanical experimental results, microscopic investigations are carried out. Figure 6 represents a polished section of the cement paste, containing a crack, so at the end of the pre-cracking phase of the specimens, without healing

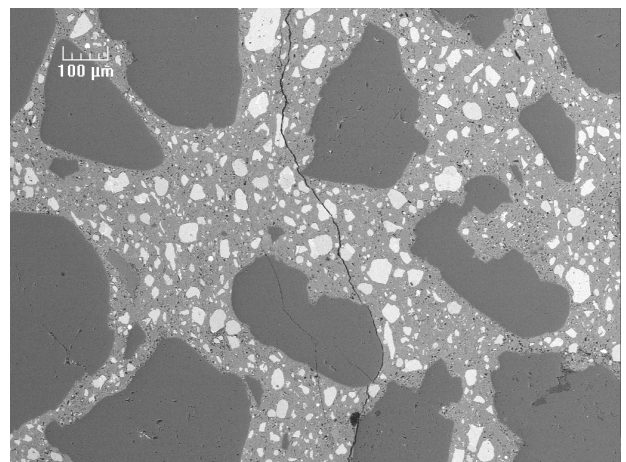


Figure 6: Cement paste of the UHPC with a crack (enlargement x100)

We can thus notice the presence of anhydrous clinker in the microstructure, which appears as white particles on figure 6 (the black ones are sand grains, and the hydration products are in grey). As already said, this illustrates the high potential of this cement for self healing. Moreover, the crack propagates in the cement paste, fracturing anhydrous grain in their whole volume or putting grains available on the crack surface. We can see this in detail on figure 7.

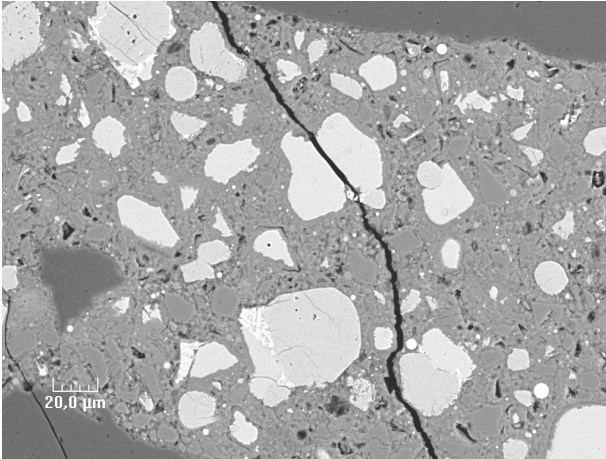


Figure 7: Propagation of the crack in and near cement grains (enlargement x500)

Similar investigations are then carried out on healed specimens. Figures 8 and 9 show that, locally, either in fractured cement grains or in the cement paste, the continuity between the two lips of the crack can be re-established. New crystals have thus precipitated in the pre-existing crack, and an energy dispersive spectrometry analysis (see an example on figure 10) demonstrates that these crystals are new C-S-H.

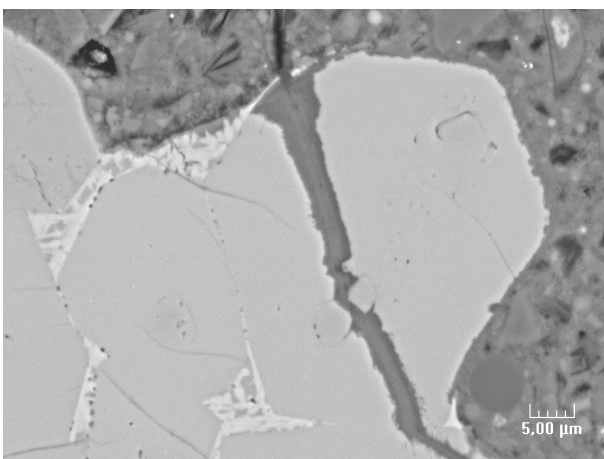


Figure 8: Precipitation of new C-S-H in a crack fracturing an anhydrous clinker grain (enlargement x2000)

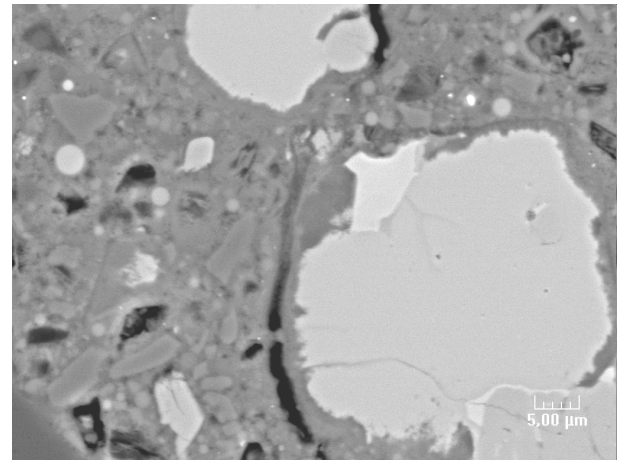


Figure 9: Precipitation of new C-S-H in a crack, outside the zone of fractured cement grain (enlargement x2000)

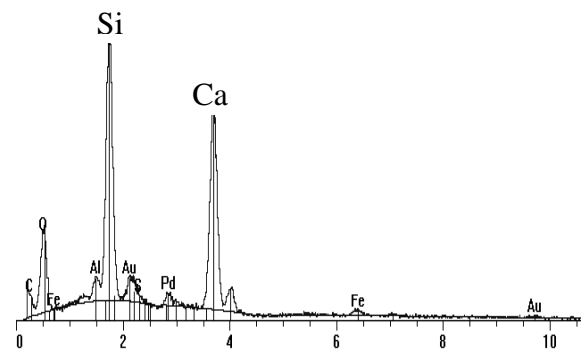


Figure 10: Result of the energy dispersive spectrometry analysis on the new crystals formed in the crack – typical spectrum of C-S-H crystals

These results make the link between the structural experimental results and what happens in the microstructure. Indeed, the fact that new links are created between the two faces of the crack enables a substantial recovery of the stiffness of the specimens. Nevertheless, this continuity is established locally, and this is why we can not have the total recovery of flexural resistance, in the sense that the material is not recreated in all the crack, and especially all the links that give its resistance to concrete.

3 A FIRST APPROACH OF MODELING

With all the information given by mechanical tests, acoustic emission analysis, and microscopic investigations, the aim of this part is now to give a first approach of modeling of the mechanical behavior of healed concrete specimens.

3.1 Elastic damage model for healthy concrete

The behavior of healthy concrete is described by an elastic damage model, which is written with the crack opening parameter. This parameter is important if we consider the fact that the crack opening has a real influence on the occurrence of the phe-

nomenon of self healing, as we have seen before. The approach presented here is one-dimensional, but could, of course, be extended.

The model is based on the crack band theory proposed by Bazant & Oh (1983). Fracture of concrete is thus represented by a band where micro-cracks appear, in a dense and distributed way. In one dimension, if we consider a bar subjected to traction, the total strain of the bar is divided in two parts: the elastic part, and the part due to cracking, as follows:

$$\varepsilon = \frac{\sigma}{E} + \frac{w}{L} \quad (1)$$

where w = the crack opening; and L = width of the crack band

In the case where the total length on the bar is equal to the width of the crack band, the elastic strain is linked to the tensile strength, and Equation 1 becomes as follows:

$$\varepsilon = \frac{f_t}{E} + \frac{w}{L} \quad (2)$$

where f_t = tensile strength

In order to link the applied stress and the crack opening in the cracking zone (fracture process zone as defined by Hillerborg et al., 1976), a fictitious crack law is used, and put in the expression of the strain. By this way, the crack opening is smeared on the total length on the bar. The parameters of the fictitious crack law (crack opening versus applied stress) are represented on figure 11.

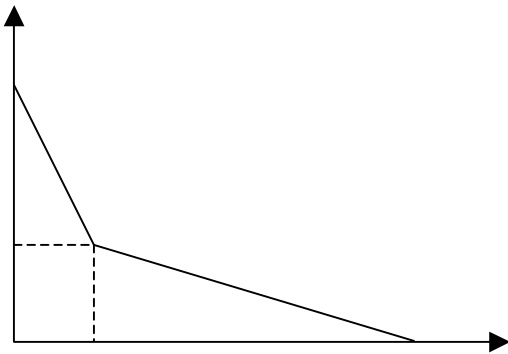


Figure 11: Parameters of the fictitious crack law

w_c is the critical crack opening when the applied stress between the two lips of the crack vanishes. f_t is the tensile strength, and the two parameters w_{int} and $f_{t,int}$ are intermediary ones. The evolution of the stress as a function of the crack opening is thus as follows:

$$\sigma = f_t - \frac{f_t - f_{t,int}}{w_{int}} w \quad \text{if} \quad 0 \leq w \leq w_{int} \quad (3)$$

$$\sigma = \frac{f_{t,int} w_{fin}}{w_{fin} - w_{int}} - \frac{f_{t,int}}{w_{fin} - w_{int}} w \quad \text{if} \quad w_{int} \leq w \leq w_{fin} \quad (4)$$

The substitution of equations 3 and 4 in equation 2 leads to the formulation of a classical scalar damage law, $\sigma = (1 - D)E\varepsilon$. The definition of the damage parameter D is thus given by the following equations:

$$D = 1 - \frac{1}{E\varepsilon} \left[f_t - \frac{f_t - f_{t,int}}{w_{int}} L \left(\varepsilon - \frac{f_t}{E} \right) \right] \quad (5)$$

if $\frac{f_t}{E} \leq \varepsilon \leq \frac{w_{int}}{L} + \frac{f_t}{E}$

$$D = 1 - \frac{1}{E\varepsilon} \frac{f_{t,int}}{w_{fin} - w_{int}} \left[w_{fin} - L \left(\varepsilon - \frac{f_t}{E} \right) \right] \quad (6)$$

if $\frac{w_{int}}{L} + \frac{f_t}{E} \leq \varepsilon \leq \frac{w_{fin}}{L} + \frac{f_t}{E}$

Loading and unloading are described by means of the loading function (in one dimension):

$$f(\varepsilon, \kappa) = \varepsilon - \kappa \quad (7)$$

where κ is a hardening-softening parameter. The initial value of κ is linked to the tensile resistance of concrete:

$$\kappa_0 = \frac{f_t}{E} \quad (8)$$

The evolution of damage is then specified as follows:

- for loading, i.e. for $f(\varepsilon, \kappa) = 0$ and $f(\varepsilon, \kappa) = 0$, then $\varepsilon = \kappa$ and D is described by equations 5 and 6.
- for unloading or reloading, i.e. for $f(\varepsilon, \kappa) \leq 0$ and $f(\varepsilon, \kappa) < 0$, then $D = 0$ and $\kappa = 0$

Unloading is performed without any residual strain, and this is one of the limitations of this first approach. The model is then implemented, only for uniaxial stress, in a finite element code using layered beam elements (see Bazant & Pijaudier-Cabot, 1987 for the principle, and Granger, 2006 for the implementation)

Three-point bending tests are simulated (see Granger, 2006 for the configuration of the simulations). Layered finite beam elements (with 15 layers) are used, and only the central element of the beam (whose width is 2 cm and corresponds to the width of the fracture process zone) is able to damage. The parameters for the damage model are presented in table 1.

Table 1. Parameters of the damage model for three-point bending tests simulations

Young modulus	42 GPa
Tensile strength	4.3 MPa
Critical crack opening (w_c)	16 μm
f_{int}	1.5 MPa
w_{int}	4 μm

The result of the simulation is presented on the figure 12, compared with two experimental tests.

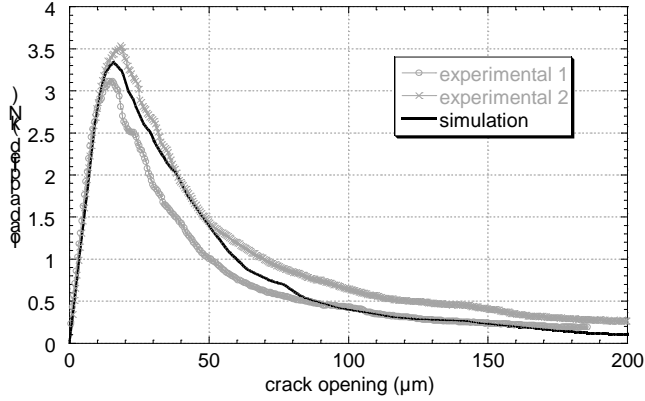


Figure 12: Simulation of three-point bending tests

The damage state of the specimens for each step of unloading in the post peak phase. Each damaged state is assumed to be one of the factor that influence the occurrence of self healing and then the recovery of structural mechanical properties.

3.2 Thermodynamics of the mechanical behavior of healed layer

Self healing appears in the damaged zone of the specimen which is represented, according to the previous section, by the damaged layers at the unloading state of the bending test simulation.

The first approach of modeling consists in introducing new mechanical properties in these damaged layers, simulating locally the effects of the self healing. New simulations will then be done considering layered finite beam elements, with layers having different mechanical behaviors (healthy, damaged or healed).

The behavior of healed layer has thus to be described in a correct thermodynamic framework. The principle is to couple an hydration model (proposed by Ulm & Coussy, 1995 and 1996), describing the evolution of properties, and a non linear mechanical behavior model, representing the fracture of concrete (the model developed in the previous section). The coupled model is described according to the local state method proposed by Lemaitre & Chaboche (1991).

3.2.1 State variables and thermodynamic potential

The layer which is going to heal is already characterized by a scalar damage variable D_1 , which is the damage state when the specimens are unloaded during the pre-cracking phase.

The evolution of healing, which is linked to hydration of anhydrous cement, can be described by the same kind of variable as the one used by Ulm & Coussy, which is called here x .

Damage during the second loading phase, is described by a second and new damage variable called D_2 .

Thus, a thermodynamic potential, relative to the healed layer, can be proposed:

$$\rho\psi = \frac{1}{2}(1-D_2)E(x).\varepsilon.\varepsilon + \frac{1}{2}(1-D_1)E.\varepsilon.\varepsilon + \left(\frac{1}{2}\kappa x^2 - A_{x_0}x\right) \quad (9)$$

where κ is a constant variable and A_{x_0} the initial chemical affinity (see Ulm & Coussy, 1995, for these parameters).

3.2.2 State equations

The state equations are then obtained by the derivation of the thermodynamic potential by the state variables:

$$\sigma = \frac{\partial\rho\psi}{\partial\varepsilon} = (1-D_2)E(x).\varepsilon + (1-D_1)E.\varepsilon \quad (10)$$

$$A_x = -\frac{\partial\rho\psi}{\partial x} = -\frac{1}{2}(1-D_2)\frac{\partial E(x)}{\partial x}.\varepsilon.\varepsilon - (\kappa x - A_{x_0}) \quad (11)$$

$$Y_1 = \frac{\partial\rho\psi}{\partial D_1} = -\frac{1}{2}E.\varepsilon.\varepsilon \quad (12)$$

$$Y_2 = \frac{\partial\rho\psi}{\partial D_2} = -\frac{1}{2}E(x).\varepsilon.\varepsilon \quad (13)$$

The first equation is the mechanical behavior law for the healed layer, which takes into account the damage of the initial healthy material (D_1) and the damage of the newly formed material (D_2). The two materials are in parallel. The mechanical properties of the first one do not evolve with healing, while the mechanical ones of the second material evolve with hydration.

Y_1 and Y_2 are the variables associated to damage and A_x the chemical affinity of the reaction of healing (as it has been described for hydration by Ulm & Coussy, 1995, 1996).

The energy dissipation, linked to the appearance of damage and to healing, writes as follows:

$$\dot{\varphi} = -\dot{D}_1 Y_1 - \dot{D}_2 Y_2 + A_x \dot{x} \quad (14)$$

Thus, including equations 11 to 13:

$$\begin{aligned} \dot{\varphi} = & \frac{1}{2} \dot{D}_1 E \varepsilon \varepsilon + \frac{1}{2} \dot{D}_2 E(x) \varepsilon \varepsilon \\ & + \left[A_{x_0} - \kappa x - \frac{1}{2} (1 - D_2) \frac{\partial E(x)}{\partial x} \varepsilon \varepsilon \right] \dot{x} \end{aligned} \quad (15)$$

Neglecting the terms where ε appears in the second order, it comes:

$$\dot{\varphi} = [A_{x_0} - \kappa x] \dot{x} \equiv A_x \dot{x} \quad (16)$$

The chemical affinity is defined so as to be positive (Ulm & Coussy, 1995). So the energy dissipation is always positive and the Clausius-Duhem principle is checked. So the thermodynamic framework, concerning the re-introduction of mechanical properties, is defined.

3.2.3 The mechanical behavior of healed material

If we now consider the state equation defined by equation 10, the mechanical behavior of the healed layer writes as follows:

$$\sigma = [E(1 - D_1) + E(x)] \varepsilon = E_c \varepsilon \quad \text{if } \varepsilon \leq \frac{f_{tc}}{E_c} \quad (17)$$

$$\sigma = E(1 - D_1) \varepsilon + (1 - D_2) E(x) \varepsilon \quad \text{if } \varepsilon > \frac{f_{tc}}{E_c} \quad (18)$$

where f_{tc} and E_c are the tensile strength and Young modulus of the healed layer, which depend on the healing variable.

So, the linear elastic part of the mechanical behavior is characterized by the new elastic modulus, depending on x and D_1 , and also related to the initial one E . We can thus define a new expression for E_c :

$$E_c = E \times (1 - D_1 + g(x, D_1)) \quad (19)$$

where g is a scalar function to be defined.

Then including equation 19 in equation 18, the mechanical behavior in the non linear part is as follows:

$$\sigma = E[(1 - D_1) + (1 - D_2)g(x, D_1)] \varepsilon \quad (20)$$

$$\sigma = [(1 - D_1 + g(x, D_1))E - D_2 g(x, D_1)E] \varepsilon \quad (21)$$

$$\sigma = E_c \left[1 - \frac{D_2 g(x, D_1)}{1 - D_1 + g(x, D_1)} \right] \varepsilon \quad (22)$$

The equation 22 can be thus assimilated to the ‘‘classical’’ form of a damage model expression, where the damage variable D_c is defined as follows:

$$D_c = \frac{D_2 g(x, D_1)}{1 - D_1 + g(x, D_1)} \quad (23)$$

So, the mechanical behavior of each layer is characterized by its tensile strength f_{tc} , its Young modulus E_c and the parameters of the damage law defined on figure 11. The evolution of damage is thus described by the equation 23. First, the new material damages, with D_2 varying from 0 to 1. When it reaches the value 1, the new material is totally damaged, and the mechanical behavior becomes the one of the initial damaged layer, with D_1 varying from its initial value after the pre-cracking phase, to 1, when the layer is totally damaged. Finally, the mechanical behavior is defined only by f_{tc} , E_c and the value of D_1 . The others parameters are then got by interpolation, in order to reach the initial behavior of the damaged layer, when D_2 is equal to 1.

3.2.4 Simulations of the bending tests

First simulations are proposed for the bending tests after healing. The initial state of damage, before the occurrence of the phenomenon, is given by the numerical result of the bending test proposed on figure 12.

After that, new mechanical properties are given to the damaged layers, and the new mechanical behaviors (damage laws) are defined, according to the section 3.2.3. All the parameters and the configuration of the tests are given in Granger (2006). The results of the simulations for 1, 3, 10 and 20 weeks healing are presented on figure 13, and compared with the experimental results on figure 14.

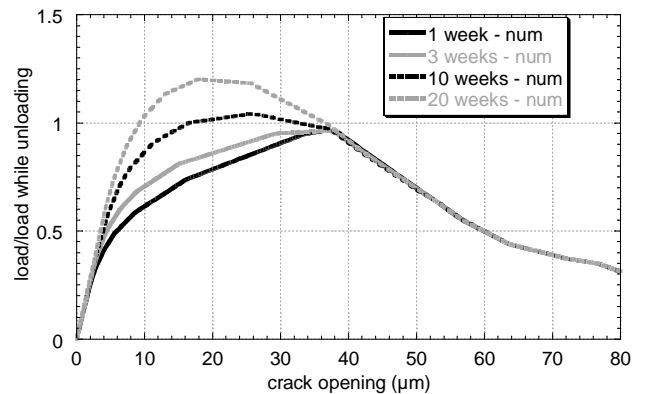


Figure 13: Numerical simulations of bending tests on healed concrete specimens (comparison with the figure 14)

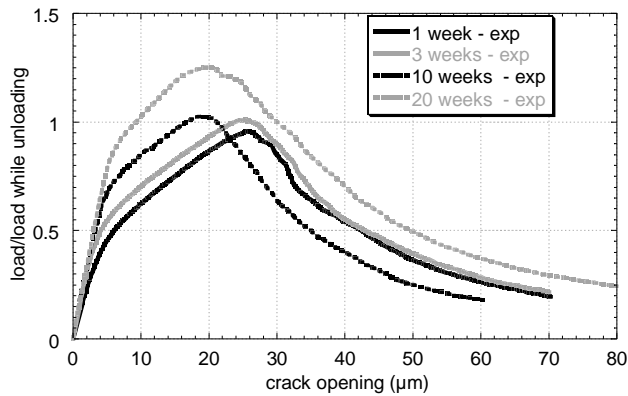


Figure 14: Experimental results of bending tests on healed concrete specimens (comparison with the figure 13)

These first simulations show that the tendencies in the pre-peak regime are quite well represented. The facts that the modeling do not take into account the residual crack opening, and that the recovery of mechanical properties is linked to the state of damage and not to the residual crack width, do not enable to represent the whole mechanical behavior of the healed specimens under three-point bending tests, and especially the post peak regime. Nevertheless, this first approach of modeling has permitted to define the thermodynamic framework and insights in order to simulate the mechanical behavior of healed specimens.

4 CONCLUSION

This research work has provided some new insights about the mechanical behavior of UHPC specimens initially cracked and then healed in water. In particular, a fast recovery of global stiffness and a light improvement of resistance have been highlighted. Experimental results have been completed by microscopic investigations which show that new crystals have precipitated in the crack.

After that, a very first approach of modeling of the mechanical behavior of healed specimens is proposed. It is based on the coupling between hydration and elastic damage models. The thermodynamics framework is thus established and first qualitative simulations are proposed, showing the experimental tendencies.

The authors want to thank the firm Lafarge, and especially the Central Research Laboratory, for its support.

REFERENCES

Bazant Z.P. & Oh B.H. 1983. Crack band theory for fracture of concrete. *Matériaux et Constructions* 16 (93): 155-177
 Bazant Z.P. & Pijaudier-Cabot G. 1987. Softening in reinforced concrete beams and frames. *Journal of Structural Engineering* 113 (12): 2333-2347

Edvardsen C. 1999. Water permeability and autogenous healing of cracks in concrete. *ACI Materials Journal* 96 (4): 448-454
 Granger S. 2006. Caractérisation expérimentale et modélisation du phénomène d'auto-cicatrisation des fissures dans les bétons. PhD thesis. Ecole Centrale de Nantes (in french)
 Granger S., Loukili A., Pijaudier-Cabot G. & Chanvillard G. 2006. Experimental characterization of the self healing of cracks in an ultra high performance cementitious material: mechanical tests and acoustic emission analysis. *Cement and Concrete Research* (2006). In press
 Hearn, N. & Morley, C.T. 1997. Self healing property of concrete – Experimental evidence. *Materials and Structures* 30: 404-411
 Hillerborg A., Modeer M. & Petersson P.E. 1976. Analysis of crack formation and crack growth in concrete by means of fracture mechanics and finite elements. *Cement and Concrete Research* 6: 773-782
 Jacobsen S., Marchand J. & Hornain H. 1995. SEM observations of the microstructure of frost deteriorated and self healed concrete. *Cement and Concrete Research* 25 (8): 55-62
 Jacobsen S., Marchand J. & Boisvert L. 1996a. Effect of cracking and healing on chloride transport in OPC concrete. *Cement and Concrete Research* 26 (6): 869-881
 Jacobsen S. & Sellevold E.J. 1996b. Self healing of high strength concrete after deterioration by freeze/thaw. *Cement and Concrete Research* 26 (1): 55-62
 Lemaitre J. & Chaboche J.L. 1991. Mécanique des matériaux solides. Paris. Dunod
 Loukili A., Richard P. & Lamirault J. 1998. A study on delayed deformations of an ultra high strength cementitious material. *ACI Recent Advances in Concrete Technology* 179: 929-949
 Neville, A. 2002. Autogenous healing – A concrete miracle? *Concrete International* November: 76-82
 Pimienta P. & Chanvillard G. 2004. Retention of the mechanical performances of Ductal® specimens kept in various aggressive environments. *Fib Symposium 2004, Avignon, 26-27 April 2004*
 Reinhardt H.W. & Joos M. 2003. Permeability and self healing of cracked concrete as a function of temperature and crack width. *Cement and Concrete Research* 33 (7): 981-985
 Ulm F.J. & Coussy O. 1995. Modeling of thermomechanical couplings of concrete at early ages. *Journal of Engineering Mechanics* 121 (7): 785-794
 Ulm F.J. & Coussy O. 1996. Strength growth as chemo-plastic hardening in early age concrete. *Journal of Engineering Mechanics* 122 (12): 1123-1132